Supporting Information

In Situ Encapsulation of Iron Oxide Nanoparticles into Nitrogen-doped Carbon Nanotubes as Anodic Electrode Materials of Lithium Ion Batteries

Ming Chen,*,[a] Feng-Ming Liu,[a] Hui Zhao,[b] Shan-Shuai Chen,[c] Xing Qian[d], Zhong-Yong Yuan[e] and Rong Wan,*,[a]

[a]*College of Chemistry and Chemical Engineering, Xinyang Normal University, Xinyang 464000, China*

[b]School of Materials Science and Engineering, Liaocheng University, Liaocheng 252000, Shandong, China

[c]Sanya Nanfan Research Institute of Hainan University, Hainan University, Sanya, 572025, China

[d]College of Chemical Engineering, Fuzhou University, Fuzhou 350116, China

[e]School of Materials Science and Engineering, Nankai University, Tianjin 300071, China

*Corresponding author. E-mail address: chenming19830618@126.com, wanrong1992@163.com

EXPERIMENTAL SECTION

Preparation of Samples.

The synthesis of C_3N_4: 10 g melamine was pressed into a pellet under a pressure of 20 MPa. The pellet was transferred to a quartz boat covered with a quartz cap and calcined at 600 °C for 0.5 h in N_2 atmosphere. Then the obtained yellow powder was collected as the carbon and nitrogen precursor for the preparation of $Fe_3C@NCNT$.

The *in situ* synthesis of $Fe_3C@NCNT$ arrays: 2 g $FeC_2O_4\cdot2H_2O$ and 5 g C_3N_4 were added to 5 mL aqueous solution under tempestuously stirring to form a yellow slurry. Then, the colloidal compounds were milled continually to form a yellow paste, following the evaporation of water. The obtained yellow paste was dried at 80 °C for 24 h and manually ground into powder. The powder was transferred to a semiclosed quartz boat and heated at 350 °C for 1 h at a heating rate of 2 °C min^{-1} in a tubular furnace under N_2 flow, and the temperature was increased to 700 °C at 2 °C min^{-1} and kept at 700 °C for 3 h, followed by cooling to room temperature naturally.

The *in situ* synthesis of $Fe_2O_3@NCNT$ arrays: The obtained $Fe_3C@NCNT$ powder was calcined in a muffle furnace in air at 300 °C for 0.5 h with a heating rate of 10 °C min^{-1}, and the final product was obtained.

The synthesis of Fe_2O_3/CB: 2 g $FeC_2O_4\cdot2H_2O$ and 0.5 g carbon black was dispersed in 3 mL deionized water and ground by mortar and pestle to form a slurry. Then the slurry was dried at 80 °C in oven overnight. The obtained powder was transferred to a quartz boat and covered by a quartz cap. Then heat treated at 300 °C for 0.5 h in air to form Fe_2O_3/CB.

Material Characterization

The crystalline structure of the products was characterized by X-ray diffraction (XRD) on a Rigaku SmartLab9 powder diffractometer equipped with Cu K_α radiation (λ =

1.541 Å). Thermogravimetric analysis (TGA) was performed on a TA SDT Q600 analyser in air with a heating rate of 10 K min^{-1}. The morphology of the products was observed by field emission scanning electron microscopy (SEM) and transmission electron microscopy (TEM). The SEM was carried out on a ZEISS SUPRA 55 microscope equipped with a secondary electron detector and the applied acceleration voltage was 3 kV. Transmission electron microscope (TEM) images and elemental mapping were taken on a Tecnai G2 F20 microscope with an accelerating voltage of 200 KV. X-ray photoelectron spectroscopy (XPS) was conducted using a Kratos Axis Ultra DLD (delay line detector) spectrometer equipped with a monochromatic Al K_α X-ray source (1486.6 eV). Raman spectra were collected on a Renishaw-1000 spectrometer by exciting a 514.5 nm Ar ion laser. N_2 adsorption-desorption isotherms were recorded at 77 K on a Quantachrome NOVA 2000e sorption analyzer. Optical absorption spectroscopy was performed in the 300-700 nm range in 1 nm steps on an ultraviolet-visible-near-infrared, double beam spectrophotometer (America PerkinElmer Lambda 950).

Electrochemical Characterization

Fe$_2$O$_3$@NCNT or Fe$_2$O$_3$/CB and polyvinylidene fluoride (PVDF) binder in a weight ratio of 9 : 1 were mixed in N-methylpyrrolidone (NMP) and stirred for 24 h to make a slurry. The slurry was then spread on a Cu foil (13 mm in diameter, 0.3 mm in thickness) with a surface density of 1.0 mg cm^{-2} (electrode thickness: 9.7 μm, Fig. S4) and dried at 120 °C for 24 h to fabricate the working electrodes in vacuum. Lithium foil was used as both the reference electrode and the counter electrode (13 mm in diameter, 0.5 mm in thickness). 1.0 M LiPF$_6$ in a 1:1 (v/v) mixture of ethylene carbonate (EC) and diethyl carbonate (DEC) was employed as the electrolyte. Celgard 2300 membrane (25 μm-thick polyethylene) was adopted as a separator. The assembly of CR2032-type coin cells was conducted in a high-purity Ar filled glovebox. Three cells were assembled in each batch for every sample and the tested average value was used for plotting the graph. Galvanostatic cycling was performed

between 0.01 and 3 V *vs* Li$^+$/Li at various C rates on a Land Battery Tester (Wuhan, China), where 1 C corresponds to 1000 mA g^{-1}. Cyclic voltammetry (CV) was conducted between 0.01 and 3 V at 0.1 mV s^{-1} using a CHI660E electrochemical workstation. Electrochemical impedance spectroscopy (EIS) was performed on the same electrochemical system over the frequency range from 100 kHz to 100 mHz with a perturbation voltage of 5 mV. The Nyquist impedance plots were fitted by Zview 2 software based on the equivalent circuit diagram. All of the electrochemical measurements were performed at 25 °C in an ambient atmosphere.
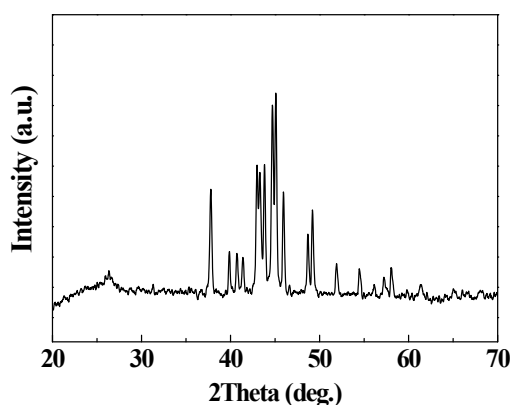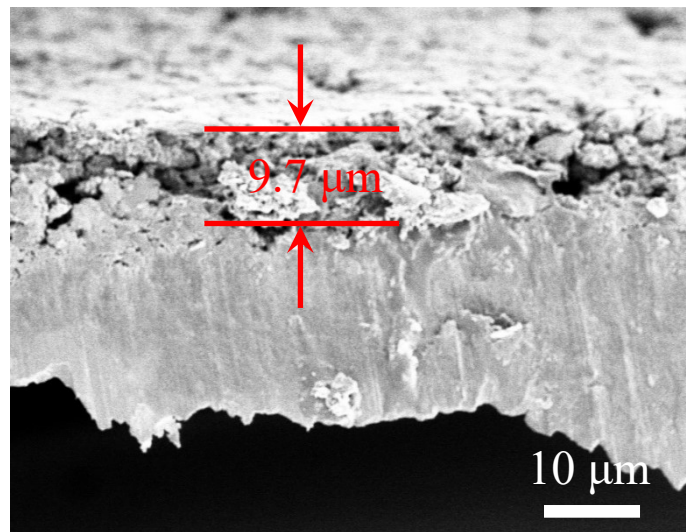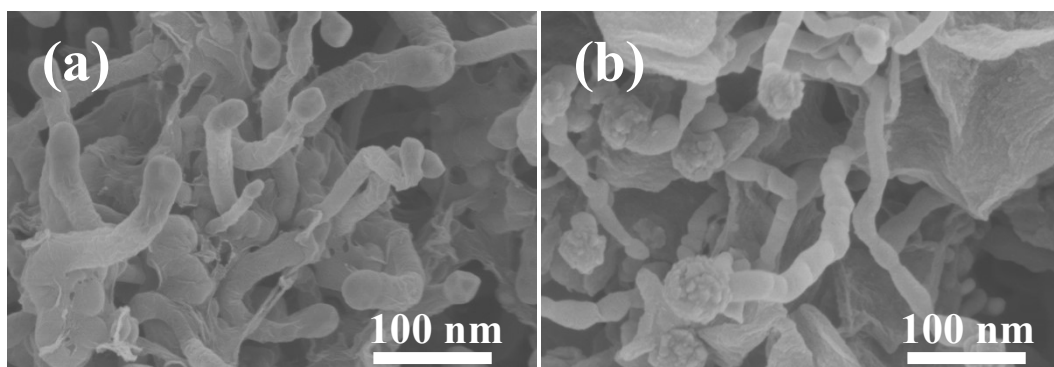

Fig. S1 XRD pattern of Fe$_3$C@NCNT
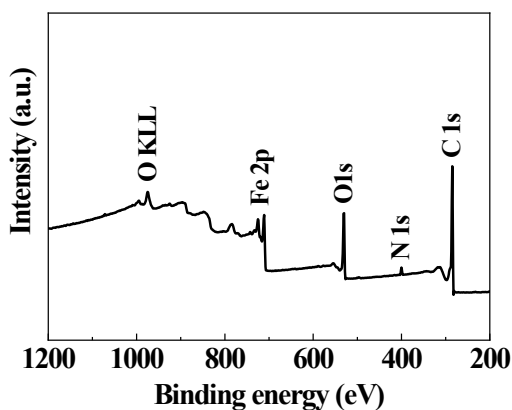
Fig. S2 XPS survey spectrum of Fe$_2$O$_3$@NCNT hybrid.
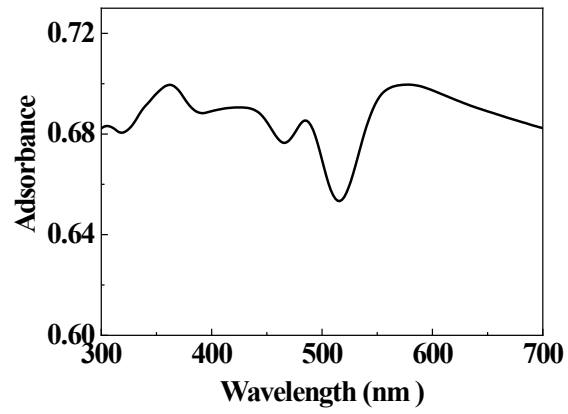
Fig. S3 Absorption spectrum of Fe_2O_3@NCNT hybrid.

Fig. S4 The cross-sectional SEM image of Fe_2O_3@NCNT electrode layer on Cu current collector.

Fig. S5 Top-view SEM images of Fe_2O_3@NCNT electrode (a) before and (b) after 800 cycles.

Table S1 Comparison of Li/Fe_2O_3@NCNT half-cell results with literature reports.

Reference	Material	Specific capacity (mAh g^{-1})	Rate-capacity (mAh g^{-1})
This work	Fe_2O_3@NCNT	0.5 C/1075 for 60 cycles	5 C/907
1	Fe_2O_3/C	0.2 C/790 for 100 cycles	4 C/390
2	Fe_2O_3/graphene	0.8 C/711 for 50 cycles	1.6 C/660
3	Fe_2O_3/graphene	0.5 C/780 for 40 cycles	2 C/420
4	Fe_2O_3/C	0.5 C/734 for 60 cycles	3 C/480
5	Fe_2O_3/Fc@SWCNT	0.5 C/650 for 25 cycles	1.2 C/550
6	YS-γ-Fe_2O_3@G-GS	0.5 C/737 for 30 cycles	5 C/443
7	Fe_2O_3/HCNF	0.2 C/816 for 100 cycles	2 C/602
8	Fe_2O_3/rGO	0.3 C/881 for 90 cycles	2 C/611
9	Fe_2O_3@CNFs	0.2 C/612 for 300 cycles	2 C/390
10	3D graphene/a-Fe_2O_3	1 C/674 for 420 cycles	5 C/336
11	HI-CNT/Fe_2O_3	0.1 C/651 for 100 cycles	5 C/420
12	γ-Fe_2O_3@graphene	1 C/833 for 100 cycles	2 C/551

References

1   H. Zhang, L. Zhou, O. N. Noonan, D. J. Martin, A. K. Whittaker, and C. Z. Yu, Tailoring the void size of iron oxide@carbon yolk-shell structure for optimized lithium storage, *Adv. Funct. Mater*., 2014, **24**, 4337-4342.

2   G. W. Zhou, J. L. Wang, P. F. Gao, X. W. Yang, Y. S. He, X. Z. Liao, J. Yang, and Z. F. Ma, Facile spray drying route for the three-dimensional graphene-encapsulated Fe_2O_3 nanoparticles for lithium ion battery anodes, *Ind. Eng. Chem. Res*., 2013, **52**, 1197-1204.

3   J. H. Wang, M. X. Gao, H. G. Pan, Y. F. Liu, Z. Zhang, J. X. Li, Q. M. Su, G. H. Du, M. Zhu, L. Z. O. Y., C. X. Shange, and Z. X. Guo, Mesoporous Fe_2O_3 flakes of high aspect ratio encased within thin carbon skeleton for superior lithium-ion battery anodes, *J. Mater. Chem. A*, 2015, **3**, 14178.

4   G. Xu, J. B. Sun, G. Y. Wang, X. F. Zhang, Z. P. Deng, L. H. Huo and S. Gao, Graphitic Carbon-Doped Mesoporous Fe_2O_3 Nanoparticles for Long Life Li-Ion Anodes, *ACS Appl. Nano Mater.*, 2021, **4**, 6689-6699.

5   J. X. Li, Y. Zhao, Y. H. Ding and L. H. Guan, Fe_2O_3 nanoparticles coated on ferrocene-encapsulated single-walled carbonnanotubes as stable anode materials for long-term cycling, *RSC Advances*, 2012, **2**, 4205-4208.

6   M. Zhang, E. Liu, T. Cao, H. Wang, C. Shi, J. Li, C. He, F. He, L. Ma and N. Zhao, Sandwiched grapheme inserted with graphene-encapsulated yolk-shell γ-Fe_2O_3 nanoparticles for efficient lithium ion storage, *J. Mater. Chem. A*, 2017, **5**, 7035-7042.

7   T. Qing, N. Q. Liu, Y. Z. Jin, G. Chen and D. Min, Helical carbon nanofibers modified with Fe_2O_3 as a high performance anode material for lithium-ion batteries, *Dalton Trans.*, 2021, **50**, 5819.

8   J. X. Zhu, T. Zhu, X. Z. Zhou, Y. Y. Zhang, X. W. Lou, X. D. Chen, H. Zhang, Huey Hoon Hng and Q. Y. Yan, Facile synthesis of metal oxide/reduced graphene oxide hybrids with high lithium storage capacity and stable cyclability, *Nanoscale*, 2011, **3**, 1084.

9   X. Y. Huang, X. Cai, D. H. Xu, W. Y. Chen, S. J. Wang, W. Y. Zhou, Y. Z. Meng, Y. P. Fang, and X. Y. Yu, Hierarchical Fe_2O_3@CNF fabric decorated with MoS_2 nanosheets as a robust anode for flexible lithium-ion batteries exhibiting ultrahigh areal capacity, *J. Mater. Chem. A*, 2018, **6**, 16890.

10 C. Z. Wang, Y. J. Zhao, X. M. Zhai, C. H. Ding, X. C. Zhao, J. B. Li, H. B. Jin, Graphene boosted pseudocapacitive lithium storage: A case of G-Fe_2O_3, *Electrochim. Acta*, 2018, **282**, 955-963.

11 S. H. Oh, O H. Kwon, Y. C. Kang, J. K. Kim and J. S. Cho, Highly integrated and interconnected CNT hybrid nanofibers decorated with a-iron oxide as freestanding anodes for flexible lithium polymer batteries, *J. Mater. Chem. A*, 2019, **7**, 12480.

12 J. T. Hu, J. X. Zheng, L. L. Tian, Y. D. Duan, L. P. Lin, S. H. Cui, H. Peng, T. C. Liu, H. Guo, X. W. Wang, and F. Pan, A core-shell nanohollow-γ-Fe_2O_3@graphene hybrid prepared through the Kirkendall process as a high performance anode material for lithium ion batteries, *Chem. Comm.*, 2015, **51**, 7855-7858.